

A Noval High Step- Up DC – DC Convertor for Renewable Energy Sources

M.Sirisha¹, B.Ravi kumar²

¹P.G.Student, Dept of EEE, AITAM Engineering College, Andhra Pradesh

²Associate Professor, Dept of EEE, AITAM Engineering College, Andhra Pradesh, sirishanaidu229@gmail.com

Abstract- The modern power systems are inter connected grid systems to maintain the reliability and power quality. The connecting of renewable energy sources power systems are very difficult to connect the grid systems, the maintenance and controlling of renewable energy sources. A 3- port dc-dc converter integrating pv and battery power for high step up application is proposed in this project. This project topology reuses switching losses by using 2 coupled inductors and 2 active clamped circuits. The couple inductor voltage stress of input side can be reduced by this new topology. 2 sets of active clamped circuits are used to recycle the energy stored in the leakage inductance and improve the system efficiency. The mode of operation doesn't need to be changed when a transition b/w charging and discharging occurs. Max power point of pv source and regulating the o/p voltage can be operated simultaneously during charging and discharging transitions. The proposed converter with fuzzy controllers has a merits of high boosting level and no of switching losses and increasing the system reliability and efficiency.

INTRODUCTION

INTEGRATED multiport converters for interfacing several power sources devices are widely used in recent years. Instead of using individual power electronic converters for Each of the energy sources, multiport converters have the advantages including less components, lower cost, more compact size and better dynamic performance. It is very important for the port connected to the energy storage to allow bidirectional power flow.

Various kinds of topologies have been proposed due to the advantages of multiport converters. The combination strategies for the multiport converter include sharing switches, capacitors, inductors, or magnetic core. One could select a proper topology by considering many aspects such as cost, reliability, and flexibility depending on the applications. An application of hybrid energy sources and storage device is shown in fig 1.

If solar power is selected as the renewable energy source and battery as the storage device, the battery can either supply the load with the solar energy at the same time or store the excess power from the solar panels for back up use. Therefore, the bidirectional power path must be provided for the battery port. It is studied that for the DC-DC converters connected to the solar panels, voltage gain extension cells such as coupled inductors, transformers, and switched capacitors are often employed to achieve high voltage conversion ratios. By utilizing the voltage gain extension cells, the extreme duty cycles that exist in typical boost converters can be avoided and the voltage stress on switches can be reduced. Thus, power switches with lower voltage rating and lower turn-on resistance can be chosen for the converters to reduce conduction losses. A converter using coupled inductors is relatively better than isolation transformers since the coupled inductors have simpler winding structure and lower conduction loss. However, the leakage

inductors of the coupled inductors will consume significant energy for a large winding ratio. In such case, the voltage stress and the loss of the switches will both be increased. A boost converter with coupled inductor and active clamp circuit is proposed. This boost converter can yield a high step-up voltage gain, reduced the voltage stress on switches and recycle the energy in the leakage inductor.

Many multiport converter topologies have been presented in the literature and can be roughly divided into two categories on this non-isolated type. The non-isolated converters are usually derived from the typical buck, boost, or buck-boost topologies and are more compact in size. The other is isolated type. The isolated converters use bridge topologies and multi-winding transformers to match wide input voltage ranges.

A topology based on buck configuration was used in space-craft front-end system. The battery port in this converter is unidirectional, so the battery cannot be charged from the photovoltaic (PV) port. The modeling of this converter is discussed but the interacting control loops are not decoupled. A multi-input buck-boost type converter is proposed to interface many renewable energy sources but there is no bidirectional port to interface the battery. A two-input converter for a hybrid fuel cell (FC)/battery power system is described with zero-voltage switching (ZVS) feature. Although the efficiency is improved, this converter could not provide a high voltage conversion ratio and bidirectional functionality. A multiple-input converter based on a boost topology is presented that has lower input current ripple and therefore is suitable for the large current applications such as hybrid vehicles. Another three-input boost converter that interfaces to unidirectional input ports and one bidirectional port is presented for a hybrid PV/FC battery system. Two types of decoupling networks are introduced based on the utilization state of the battery. A multi-input single-ended primary-inductor converter with a bidirectional input is proposed in this converter is suitable for the hybrid system that incorporates energy storage elements such as ultra-capacitors. However, lack of voltage gain extension cells makes the converters difficult to be used in high step-up applications. Moreover, for the converters in and, the operation mode has to be changed after a transition between charging and discharging occurs. This would increase the complexity of the control scheme and might reduce the reliability of the system.

A time-sharing multiple-input converter using active clamping technique is proposed. The converter provides two isolated ports, which is overqualified for our application. Bidirectional port can be added into this time-sharing converter to form an isolated three-port converter but the power stage and the control scheme will become complicated. Many isolated three-port converters with half-bridge or full-bridge topologies are suitable for high step-up applications since a multi-winding transformer is adopted. These isolated three-port converters could achieve galvanic isolation and bidirectional capabilities but the amount of active switches results in complicated driving circuits and large size. A converter based on the boost-dual-half-bridge topology is pre-compensated. This converter is composed of three half-bridges and a three-winding transformer and is suitable for high step-up applications. However, the amount of active switches, input inductors, and filter capacitors would increase the cost and size of the converter. Another three-port triple-half-bridge converter using a combined phase-shift and PWM control to manage the bidirectional power flow is present. However, the same duty cycle is given to all three half-bridges and is only variable regulating the voltage level. Therefore, this converter can only be used in the applications where single power source

or storage element is connected unless additional voltage control loop that allows different duty cycle is introduced. A converter utilizing flux additively in a multi-winding transformer is presented. Although this topology can simultaneously transfer power from different ports, the reverse blocking diodes only allow unidirectional power flow; therefore, the converter is not suitable for applications that required energy storage elements. In a three-port bi-directional converter with three active full bridges, a three-

winding transformer and two series resonant tank is reported. The transformer provides full isolation among all ports and wide input voltage range. The switching losses are reduced due to soft switching operation. The full bridge topology is good for relative high power application but requires more power switches and complicated circuit design. Integrated three port converters derived from a half-bridge converter are presented in to interface PV and battery power. Small signal modeling and decoupling network is introduced in to design the compensators separately for the cross coupled control loops. A family of three –port half bridge converters is described in and the primary circuit can function as a synchronous rectification buck converter. Therefore, the converters in are suitable for stand - alone step –down applications. Many other multi- input topologies are discussed.

In this paper ,a high step – up three port dc-dc converter for the hybrid PV/battery system is proposed with the following advantages : 1) High voltage conversion ratio is achieved by using coupled inductors . 2) Simple converter topology which has reduce the number of the switches and associate circuits. 3) Simple control energy which does not need to change the operation mode after a charging/ discharging transition occurs unless the charging voltage is too high. 4) Output voltage is always regulated at 380 V under all operation modes. It is noted that for the MPP- tracking converters, operating range has to be limiting the operating range of the converter in the voltages higher than MPP.

Studies show that a solar panel converts 30-40% of energy incident on it to electrical energy. A Maximum Power Point Tracking algorithm is necessary to increase the efficiency of the solar Panel.

There are different techniques for MPPT such as Perturb and Observe (hill climbing method), Incremental conductance, Fractional Short Circuit Current, Fractional Open Circuit Voltage, Fuzzy Control, Neural Network Control etc. Among all the methods Perturb and observe (P&O) and Incremental conductance are most commonly used because of their simple implementation, Lesser time to track the MPP and several other economic reasons.

Under abruptly changing weather conditions (irradiance level) as MPP changes continuously, P&O takes it as a change in MPP due to perturbation rather than that of irradiance and Sometimes ends up in calculating wrong MPP. However this problem gets avoided in Incremental Conductance method as the algorithm takes two samples of voltage and current to calculate MPP. However, instead of higher efficiency the complexity of the algorithm is very High compared to the previous one and hence the cost of implementation increases. So we have to mitigate with a tradeoff between complexity and efficiency. It is seen that the efficiency of the system also depends upon the converter. Typically it is Maximum for a buck topology, then for buck-boost topology and minimum for a boost topology. When multiple solar modules are connected in parallel, another analog technique TEODI is also Very effective which operates on the principle of equalization of output operating points incorrespondence to force displacement of input operating points of the identical operating system.

It is very simple to implement and has high efficiency both under stationary and time varying atmospheric conditions .

As shown in Fig 1, comparing to the typical multi converter configuration that requires individual microcontroller for each converter, the integrated three- port converters are controlled by a single microcontroller. The communication interface utilized in the multi converter configuration could be removed due to

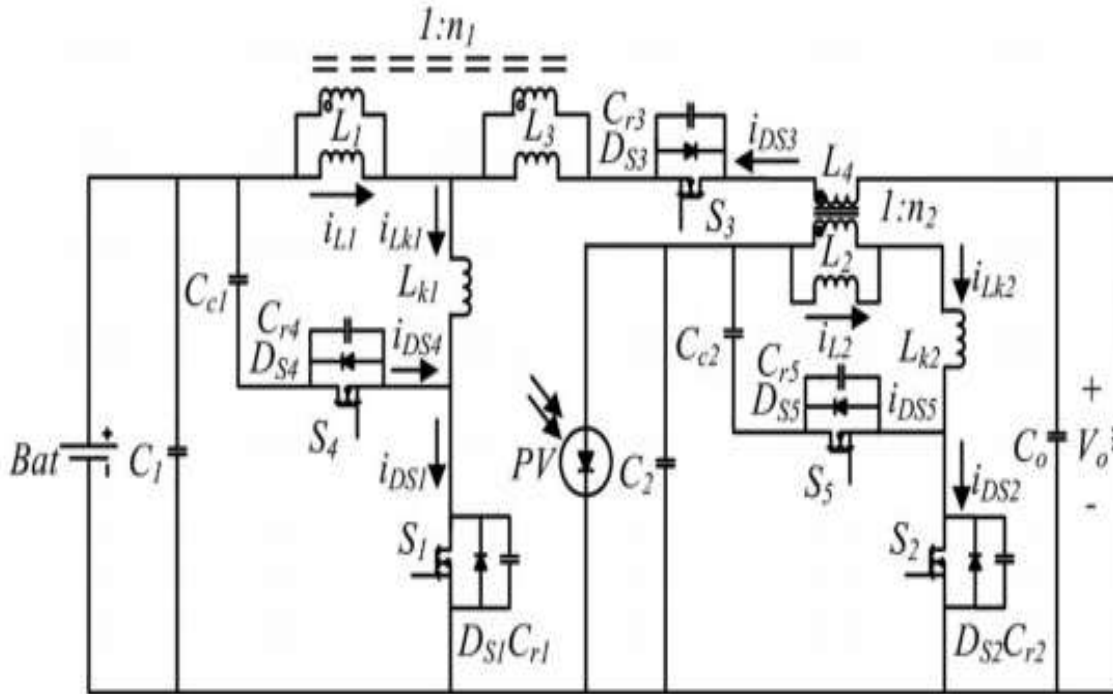


Fig 1. Topology of the proposed converter

Centralized control of the proposed converter. Therefore, the system cost and volume can be reduced. The major contribution of this paper is to propose an integrated three – port converter as a non isolated alternative other than typical isolated topologies for high step –up three port applications. The proposed switching strategy allows the converter to be control by the same two duty cycles in different operation modes. The detailed analysis is given in the following sections: The principle of operation is described in section II. The PV source modeling, topological modes, and ZVS conditions are analyzed in section III. The modeling and control strategy is explained in section IV. Finally, the experimental results are presented in section V.

II . PRINCIPLE OF OPERATION

This section introduces the topology of proposed non isolated three-port dc–dc converter, as illustrated in Fig. 2. The converter is composed of two main switches S_1 and S_2 for the battery and PV port. Synchronous switch S_3 is driven complementarily to S_1 such that bidirectional power flow for the battery port can be achieved. Two coupled inductors with winding ratios n_1 and n_2 are used as voltage gain extension cells. Two sets of active-clamp circuits formed by S_4, L_{k1}, C_{c1} and S_5, L_{k2}, C_{c2} are used to recycle the leakage energy. L_{k1} and L_{k2} are both composed of a small leakage inductor from the coupled inductor and an external leakage inductor. Two independent control variables, duty cycles d_1 and d_2 , allow the control over two ports of the converter, while the third port is for the power balance. The fixed-frequency driving signals of the auxiliary switches S_3 and S_4 are complementary to primary

switch S_1 . Again, S_3 provides a bidirectional path for the battery port. Similarly, S_5 is driven in a complementary manner to S_2 . A 180° phase shift is applied between the driving signals of S_1 and S_2 . There are four operation periods based on the available solar power. First, the sun is in the eclipse stage and the solar irradiation is either unavailable or very low. This operation period is defined as period 1, and the battery will serve as the main power source. As the sun starts to shine and the initial solar irradiation is enough for supplying part of the load demand, the operation period is changed to period 2. The load is supplied by both solar and battery power in this period. For period 3, the increasing isolation makes the solar power larger than the load demand. The battery will preserve extra solar power for backup use. During period 4, the charging voltage of the battery reaches the preset level and should be limited to prevent overcharging. According to the solar irradiation and the load demand, the proposed three-port converter can be operated under two modes. In the battery balance mode (mode 1), maximum power point tracking (MPPT) is always operated for the PV port to draw maximum power from the solar panels. The battery port will maintain the power balance by storing the unconsumed solar power during light-load condition or providing the power deficit during heavy-load condition. The power sharing of the inputs can be represented as

$$P_{load} = P_{pv\ SVC} + P_{bat\ SVC} \quad (1)$$

where P_{load} is the load demand power, $P_{pv\ SVC}$ is the PV power under solar voltage control (SVC), and $P_{bat\ SVC}$ is the battery power under SVC. In mode 1, maximum power is drawn from the PV source. The battery may provide or absorb power depending on the load demand. Therefore, $P_{bat\ SVC}$ could be either positive or negative. When the battery charging voltage is higher than the maximum setting, the converter will be switched into battery management mode (mode 2). In mode 2, MPPT will be disabled; therefore, only part of the solar power is drawn.

However, the battery voltage could be controlled to protect the battery from overcharging. The power sharing of the inputs can be represented as

$$P_{load} = P_{pv\ BVC} + P_{bat\ BVC} \quad (2)$$

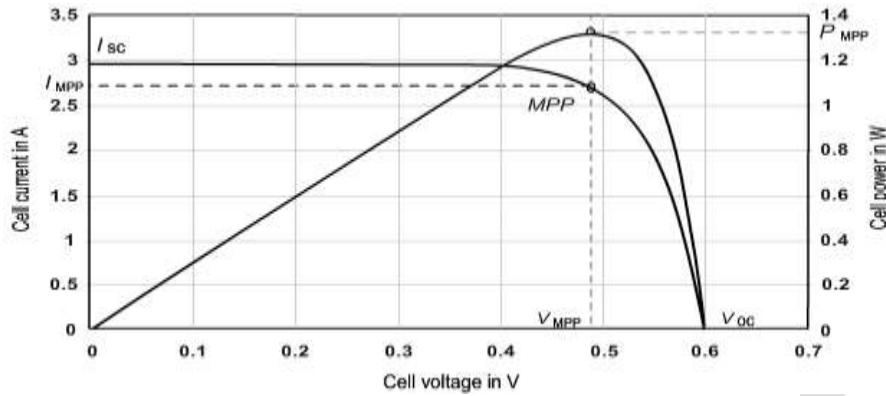
where $P_{pv\ BVC}$ is the PV power under battery voltage control (BVC) and $P_{bat\ BVC}$ is the battery charging power under SVC. If the load is increased and the battery voltage is reduced, the converter will be switched to mode 1. The output voltage is always kept at 380 V in both modes.

III TOPOLOGICAL MODES AND ANALYSIS

A) PV Source Modeling

It is well explained in the literature that using a PV generator as input source has significant effect on the converter dynamics. The non linear $V-I$ characteristics of a PV generator can be modeled using current source, diode, and resistors. The single-diode model is used for the PV source modeling. This model provides a tradeoff between accuracy and complexity. A solar cell is the building block of a solar panel. A photovoltaic module is formed by connecting many solar cells in series and parallel. Considering only a single solar cell; it can be modeled by utilizing a current source, a diode and two resistors. This model is known as a single diode model of solar cell. Two diode models are also available but only single diode model is considered here

$$I = N_p * I_{lg} - N_p * I_{os} * \left[\exp \left\{ q * \frac{V + I * R_s}{A * K * T} \right\} - 1 \right] - \frac{V * \left(\frac{N_p}{N_s} \right) + I * R_s}{R_{sh}}$$



The I-V and P-V curves for a solar cell are given in the following figure. It can be seen that the cell operates as a constant current source at low values of operating voltages and a constant voltage source at low values of operating current.

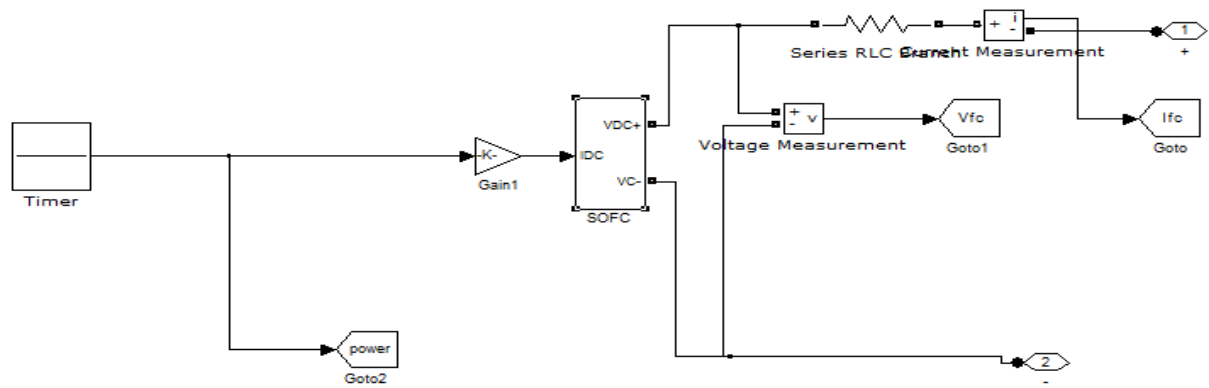


Fig: 2 PV Cell

B) Operation of the Topological modes

Before performing the analysis, some assumptions should be made: 1) the switches are assumed to be ideal ; 2) the magnetizing inductors are large enough so that the current flowing through the inductors is constant ; 3) the capacitors are large enough so that the voltages across the capacitors are constant .

Mode 1: S_1 is auxiliary switches S_4 and S_5 are turn OFF, while primary switch S_2 turned ON. Although S_1 is the off state, resonant inductor L_{k1} resonates with C_{r1} and C_{r4} . In this period , C_{r1} is discharged to zero and C_{r4} is charged to $V_{bat} + V_{C_{c1}}$. For the PV port, S_2 is turned ON and the current from the PV panels flow through $V_{pv-th} - L_2 - L_{k2} - S_2$ loop. In order to achieve the ZVS feature for S_1 , the energy stored in resonant inductor L_{k1} should satisfy the following inequality:

$$L_{k1} \geq \frac{\left(\frac{C_{r1}}{C_{r4}}\right)V_{Ds1}(t_0)^2}{i_{Lk1}(t_0)^2}$$

Mode 2 : S_1 begins to conduct current at t_2 and the battery port current follows the path $V_{bat} - L_1 - L_{k1} - S_1$. S_2 is also turn ON in this interval. Therefore, both L_1 and L_2 are linearly charged and energy of both input ports is stored in these magnetizing inductors. Auxiliary switches S_3 , S_4 , and S_5 are all turned OFF. S_2 starts to be turned OFF and the auxiliary switch S_5 remains in the OFF state. However, a resonant circuit formed by L_{k2} , C_{r2} and C_{r5} release the energy stored in L_{k2}

$$L_{k2} \geq \frac{\left(\frac{C_{r2}}{C_{r5}}\right)V_{Ds2}(t_2)^2}{i_{Lk1}(t_2)^2}$$

Mode 3 : At t_5 , the current of L_{k2} is reversed in direction and energy stored in t_5 is released through the $C_{c2} - S_5 - L_{k2} - L_3$ loop. This interval ends when S_5 is turned OFF. Switches S_2 and S_5 are both in the off state at t_6 . A resonant circuit is performed by L_{k2} , C_{r2} , and C_{r5} . During this interval, C_{r2} is discharge to zero and C_{r5} is charged to $V_{pv-th} + V_{Cc2}$. The energy stored in L_{k2} should be greater than the energy stored in parasitic capacitors $Cr2$ and $Cr5$

$$L_{k2} \geq \frac{\left(\frac{C_{r2}}{C_{r5}}\right)V_{Ds2}(t_{63})^2}{i_{Lk1}(t_3)^2}$$

Mode 4 : At S_1 is turned OFF while S_3 and S_4 remain in OFF state. During this interval, L_{k1} will resonant with C_{r1} and C_{r4} to release the energy trapped in it. Resonant capacitor C_{r1} is charged to $V_{bat} + V_{Cc1}$, while C_{r4} is discharge to zero, The energy stored in leakage inductor L_{k2} should satisfy the following inequality. The current flow through L_{k1} , and energy stored in

$$L_{k1} \geq \frac{\left(\frac{C_{r1}}{C_{r4}}\right)V_{Ds2}(t_4)^2}{i_{Lk1}(t_4)^2}$$

IV . Control Strategy

As mentioned in section II, the operation modes of the converter are determined by the conditions of available solar power and battery charging. Controlling the converter in each mode requires different state variables to regulate voltages of the input and output ports. There are three control loops for the proposed converter: Output voltage control (OVC), solar voltage control (SVC), battery control (BVC). The OVC is a simple voltage regulation loop. SVC will be disabled immediately to avoid the noise issue caused by the MPPT algorithm. Fuzzy controller is used in this paper. To determine the appropriate Amount of tip requires mapping inputs to the appropriate outputs. Membership functions for creating fuzzy inference systems, support for AND, OR, and NOT logic in user-define rules. Standard Mamdani and Sugeno-type fuzzy inference systems. The ruler viewer and the surface viewer are used for looking at, as opposed to editing, the FIS. They are strictly read- only tools.

RULES TABLE

COE E	NB	NM	NS	ZE	PS	PM	PB
NB	NB	NB	NB	NB	NM	NS	ZE
NM	NB	NB	NB	NM	NS	ZE	PS

NS	NB	NM	NS	NS	ZE	PS	PM
ZE	NB	NM	NS	ZE	PB	NS	ZE
PS	NM	NS	ZE	PS	PM	PM	PB
PM	NS	ZE	PS	PM	PB	PB	PB
PB	ZE	PS	PM	PB	PB	PB	PB

TABLE I

Circuit Parameters

Parameter	Value
V_{bat}	
$V_{pv-oc} (800W/m^2)$	48V
V_o	52.8 V
P_{pv-max}	380V
P^{o-max}	200W
f_{sw}	200W
n_1, n_2	50KHz
L_1, L_2	4.44
L_{k1}, L_{k2}	52 μ H
C_{c1}, C_{c2}	1 μ H
C_o	470 μ F
	47 μ F

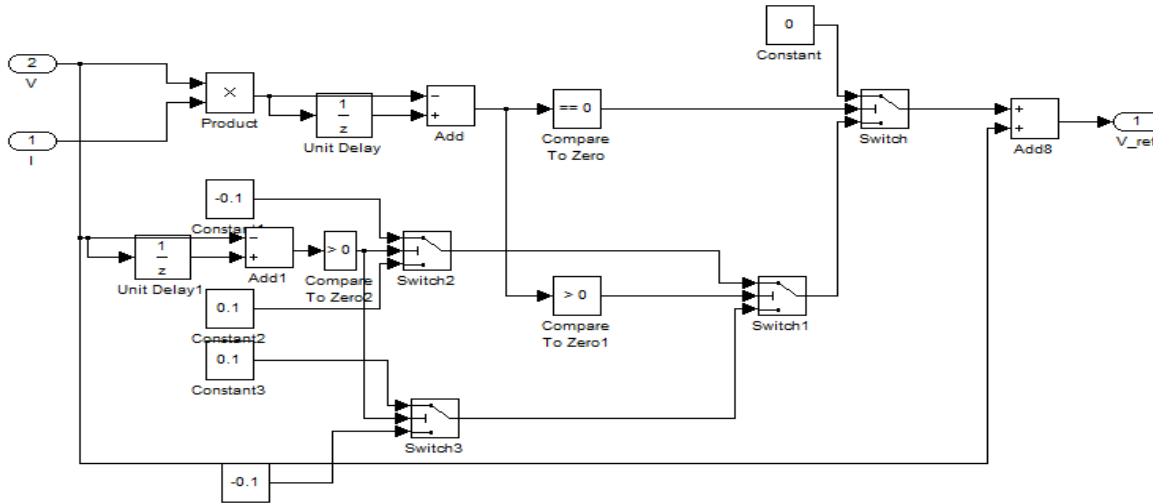


Fig: 3 Perturb and Observe technique

V EXPERIMENTAL RESULTS

In fig a , the sun radiation is in period 1 . for the 40 s , there is very little sunlight, so the MPPT is performed. however ,once the level is too low or not available ,MPPT is then disabled and the battery will become the only power source to supply the load . In fig . b, the sun radiation is period 2 . The solar port is operated under MPPT and the battery port is discharged to supply part of the load. As the irradiation increases, the PV port will generate more power than the battery port. The increasing sun radiation reaches period 3 in fig c. The power generated from the PV port is now larger than the load demand, so the battery port should be charged to store additional power. Although the batteries are charged, the charging voltage is not high enough the trigger the BVC loop. Thus, the solar panels still work under MPPT. As shown fig d. the maximum power and the deficit is provided by the batteries is reached in period 4. The BVC loop is then active to regulate the charging voltage and the MPPT is disabled.

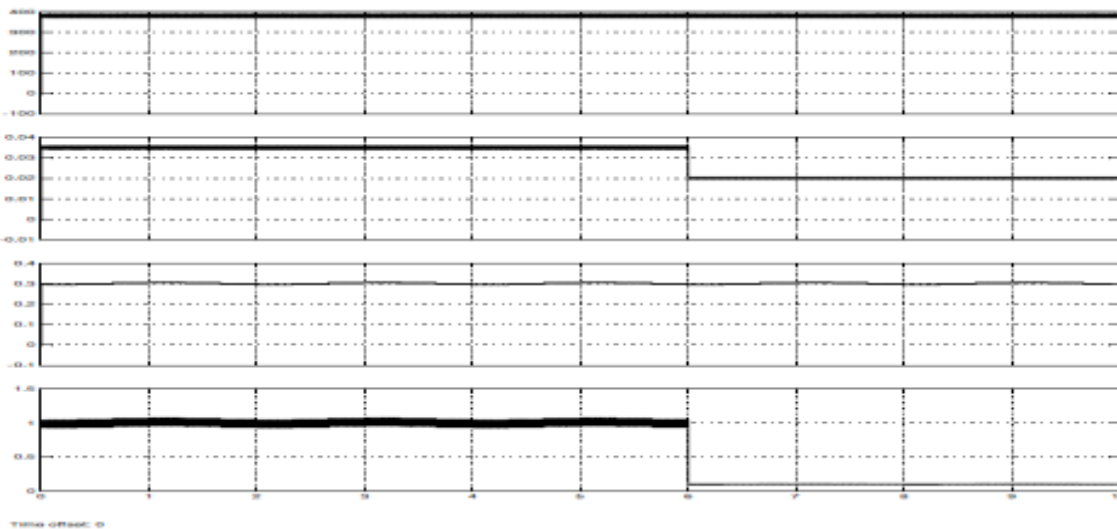


Fig.3 Measured waveforms of mode operation in period 1 ($R = 3030\Omega$, Ch 1 : V_0 , Ch 2 : V_b , Ch 3: I_b , Ch 4: I_{pv})

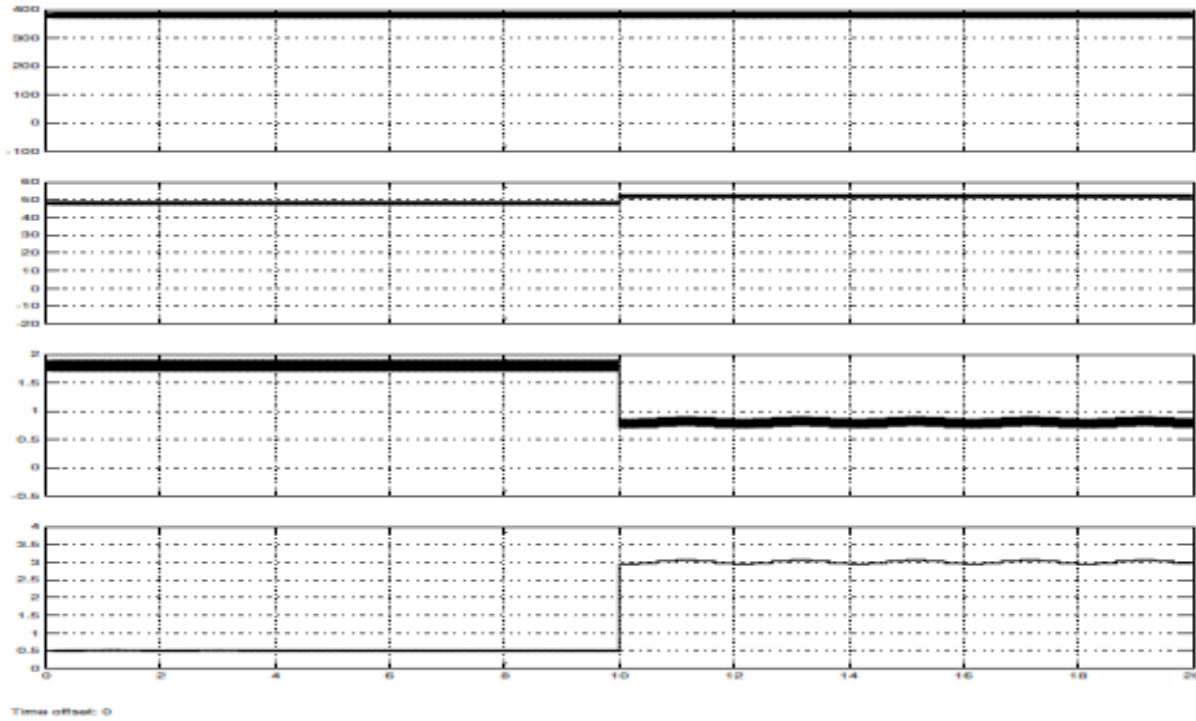


Fig.4 Measured waveforms of mode operation in period 2 (a) Lower Solar irradiation level (b) Higher Solar irradiation level ($R=1204 \Omega$, Ch1: V_o , Ch2: V_b , Ch 3: I_b , Ch4: I_{pv})

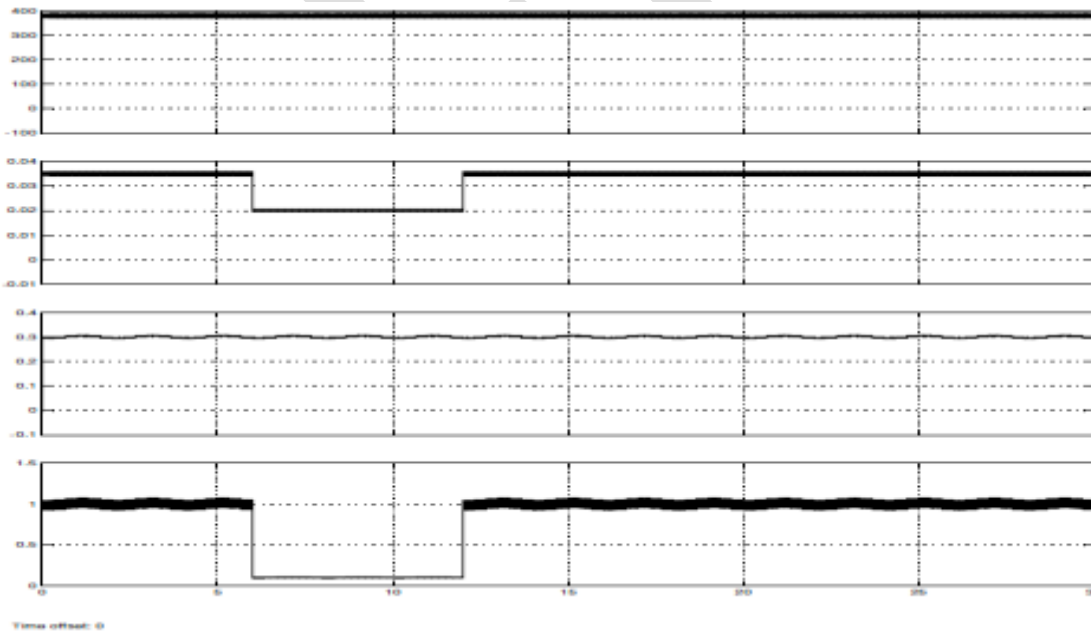


Fig.5 Measured waveforms of mode operation in period 3 ($R = 3030 \Omega$ Ch1: V_o , Ch2: V_b , Ch 3: I_b , Ch4: I_{pv})

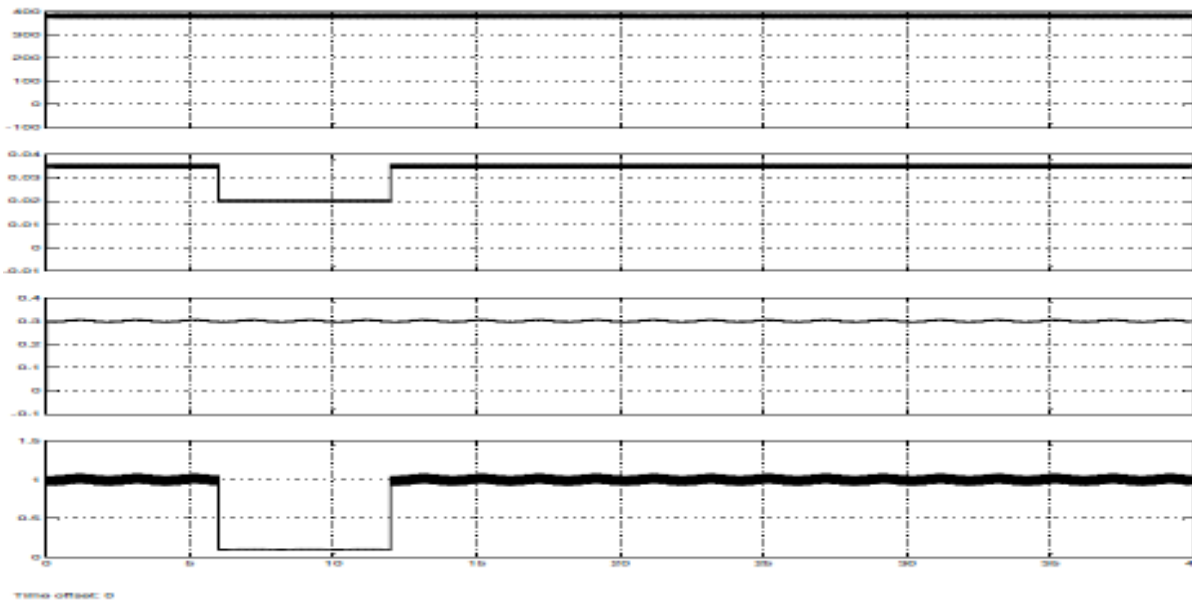


Fig.6 Measured waveforms of mode operation in period 4 ($R = 3030 \Omega$ Ch1: V_o , Ch2: V_b , Ch 3: I_b , Ch4: I_{pv})

VI. CONCLUSION

A novel high step – up three port DC – DC converter for renewable energy source is proposed to integrate solar and battery power. In this topology , two coupled inductors are used for high voltage output, and active – clamping circuits are used to recycle the energy to store the leakage inductors. Fuzzy techniques was used for controlling in this paper. Two duty ratios in different operation modes by using switching strategy. The experimental results proposed converter under different solar radiation levels. The battery could be achieved without changing the operation mode; so the MPPT technique will not be interrupted. In light – load condition, once the charging voltage is higher than the preset level, the operation mode will be changed rapidly to protect the battery from overcharging. The highest converter efficiency is measured as 90.5% at 110w.

REFERENCES:

- [1] Proc. IEEE Int. Symp. Circuits Syst. (ISCAS), 2003, vol. 3, pp, 435-438 H. Chung and Y.K Mock, “ Development of a Switched-capacitor dc-dc boost converter with continuous input current waveform”
- [2] no.2, pp.217-225, March. 2005. Q. Zhao and F.C. Lee, “ High- efficiency, high step – up dc-dc converters,” IEEE Trans. Power Electron., vol.18, no.1, pp . 65-73
- [3] March 2009 J.W. Back, M. H. Ryoo, T. J. Kim, D. W. Yoo, and J. S. Kim, “High boost converter using voltage multiplier,” in Proc. IEEE Ind.
- [4] R. J. Wai, C. Y. Lin, R. Y. Duan, and Y.R. Chang, “ High – efficiency dc-dc converter with high voltage gain and reduced and reduced switch stress, “IEEE Trans. Ind. Electron, vol. 54, no . 1, pp. 354 – 364
- [5] S.M. Chen, T. J. Liang, L. S. Yang, and J. F. Chen, “ A cascaded high step – up dc-dc converter with single switch for micro source applications,” IEEE Trans . Power Electron. , vol. 26, no. 4, pp. 1146-1153, Apr. 2011
- [6] Yeong-Chau Kuo, al “Novel Maximum Power-Point-Tracking Photovoltaic Energy Conversion System. “ IEEE Transaction on Industrial Electronics, vol. 48, no. 3 June 2001, PP 594-601

- [7] Hu, Yaoming, "Nonlinear Control System Theory and Application." National Defense Industry Press, January 2002
- [8] HikeHiko Sugimoto et al "A New scheme for Maximum Photovoltaic Power Tracking control" Preceding of Power conversion conference, vo 1.2 , PP 691-696 Ngaaka 1997
- [9] Lin Shan etc. "Tracking and Control of Maximum Power Point or Photovoltaic System New Energy Source, 1991 vo 1.21, No.2 P2.5-21
- [10] N. Femia, G. Lisi, G. Petrone Spagnuolo and M Vitelli, "m Distributed Maximum Power Point Tracking of Photovoltaic array Novel approach and Analysis" IEEE Trans on Ind . Electron vol.56 No.5 2006
- [11] J. Jung and A. Kaminski, "A multiple-input SEPIC with a bi-directional input for modular distributed generation and energy storage integration," in Proc.IEEE Appl.Power Electron. Conf, 2011, PP. 28-34.
- [12] G. J. Su and F. Z. Peng, " A Low cost, triple- voltage bus dc-dc converter for automotive applications," in proc. IEEE Appl., Power Electron. Conf., 2005, pp. 1015-1021.
- [13] A.Kwasinski, "Identification of feasible topologies for multiple-input dc-dc converters," IEEE Trans. Power Electron., vol 24, no.3 , pp.856-861, Mar. 2009.
- [14] S.Yu and A.Kwasinski, " Analysis of a soft-switching technique for isolated time-sharing multiple input converters," in proc.IEEE Appl.Power Electron. Conf., 2012, pp.844-851.
- [15] D.Lin and H. Li, "A ZVS bidirectional dc-dc converter for multiple energy storage elements," IEEE Trans.Power Electron., vol.21, no.5, pp. 1513-1517, Sep. 2006.
- [16] H.Tao A.Kotsopoulouendrix, "Triple-half-bridge bidirectional converter controlled by phase shift and PWM," in proc. IEEE Appl. Power Electron. Conf., Mar.2006, PP.1256-1262
- [17] L.Wang, Z. Wang and H.Li, " Asymmetrical duty cycle control and decoupled power flow design of a three-port bidirectional DC-DC converter for fuel cell vehicle application ?," IEEE Trans. Power Electron., vol.27 no.2, PP . 891-903, Feb .2012.
- [18] Y.-M. Chen, Y-C. Liu, and F-Y. Wu, " Multi-input DC/DC converter based on the multiwinding transformer for renewable energy applications," IEEE Trans.Lnd.Appl., vol.38, no.4, pp.1096-1104, jul/Aug.2002.
- [19] H.Tao, A.Kotsopoulos, J.L.Durate, and M.A.M.Hendrix, "Transformed coupled multiport ZVS bidirectional DC-DC converter with wide input range," IEEE trans.Power Electron., vol.23, no.2, pp.771-781, Mar.2008.
- [20] TSunito, J.Leppaaho, J.Huusari, and L.Nousiainen, "Issue on Solar- generator interfacing with current-fed MPP-tracking converters," IEEE Trans.Power Electron., vol.25, no.9, pp.2409-2419, Sep.2010
- [21] J.Gow and C.Manning, "Development of a Photovoltaic array model for use in power electronics simulation studies," IEEE Proc.Electric Power Appl., vol.146, no.6, pp. 193-200, 2002